SIMULATED INTERGRANULAR FRACTURE CHARACTERISTICS

P. PONÍŽIL AND I. SAXL

Faculty of Technology, Tomas Bata University, Zlín
Mathematical Institute, Acad. Sci. of the Czech Republic, Praha

ABSTRACT

The recently proposed spatial model of the intergranular crack propagation was applied to models of grain structure represented by Voronoi tesselations generated by various point processes producing substantially different cell size distributions.

Statistical properties of the individual features composing the fracture surface and different roughness parameters of the simulated crack have been examined and their sensitivity to the3D structural characteristics was tested. Finally, the models of the relation between characteristics of fracture lines and surface roughness were critically examined.

INTRODUCTION

A study of the computer simulated intergranular crack propagation in grain structures modelled by Voronoi tessellations of different types was described in [1]. It was based on the model proposed by Šandera et al. [2] for the subcritical crack development within the process zone at the tip of the fatigue precrack. The selected Voronoi tessellations covered a wide range of grain structures from a nearly isohedral tiling to a dispersed cell structure formed by regions of small cell separated by cells of approximately 70times greater volume v (CV $v \approx 4.5$). The fracture lines along the crack propagation direction and perpendicular to it were analysed together with the whole fracture surface with the following results: the first order geometric characteristics of fracture features (*i.e.* mean lengths $\mathbf{E}l$ of fracture line segments, linear roughness R_L, mean area $\mathbf{E}a$ of fractured facets, mean number of their vertices, mean perimeter, mean orientation and surface roughness R_S) are only weakly affected by the underlying cell structure and a rather detailed investigation covering at least about 10^3 features is necessary to detect some effect of the cell structure. On the other hand, the second order quantities, like variances of the geometric cell characteristics or their coefficients of variances are much more structure sensitive as demonstrates Tab. 1., in which the ratios of maximum and minimum values observed in the five examined fractured cell systems are compared.

Tab. 1. Ratios of maximum and minimum observed values

	CV v	$\mathbf{E}l$	CV l	$\mathbf{E}a$	CV a	R_L	CV R_L	R_S	CV R_S
$\frac{\max\bullet}{\min\bullet}$	1125	1.17	2.1	1.2	5.4	1.1	2.2	1.1	3.9

Several quantities have their extremes at the mildly random cell structure of the Poisson-Voronoi tessellation (CV $v = 0.42$), hence the fracture characteristic are not monotone functions of CV v or of another characteristics of the cell size dispersion.

In the present paper, the above mentioned study is extended to other roughness parameters characterizing the fracture surface in a more detailed manner than linear and surface roughnesses. As the medium of the fracture propagation, three unit space filling cell (grain) systems have been chosen (for details see [1], the mean cell volume $\mathbf{E}v = 1$ in a unit tessellation):

a) slightly perturbed dodecahedral tiling generated by the Bookstein model on the fcc lattice denoted by Bcf0.005 (0.005 is the standard deviation a of 3D normal $N(0,a^2I)$ distribution of the i.i.d. distributed node shifts of the unit face-centred cubic lattice),

b) Poisson-Voronoi tessellation (PVT),

c) tessellations generated by the Bernoulli cluster field with spherical and globular clusters (embedding sphere diameter $\delta = 0.05$) and the mean cluster cardinality $N = 70$ (notation BePS70, BePG70.

The 2D sections of examined models shows Fig. 1.

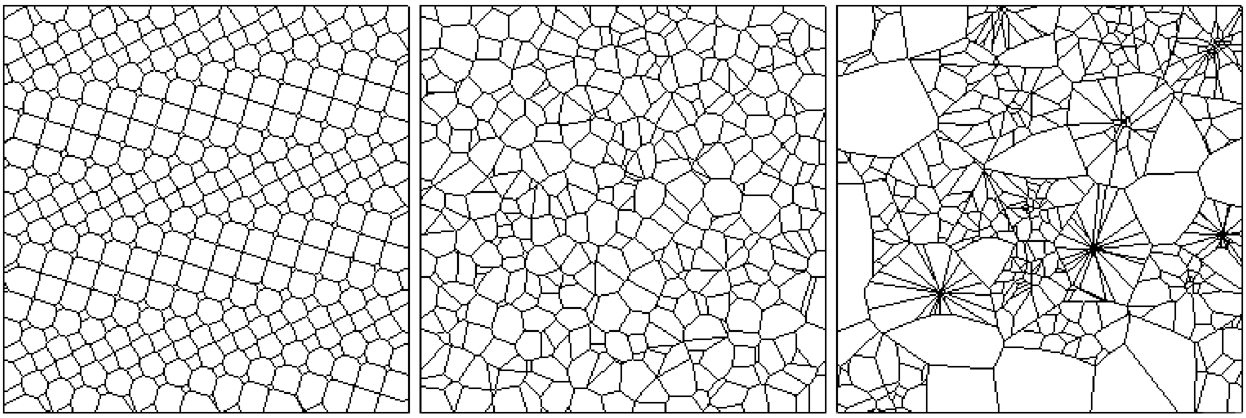

Bcf0.005 PVT BePS70

Fig. 1 2D sections of examined models.

ROUGHNESS INDICES

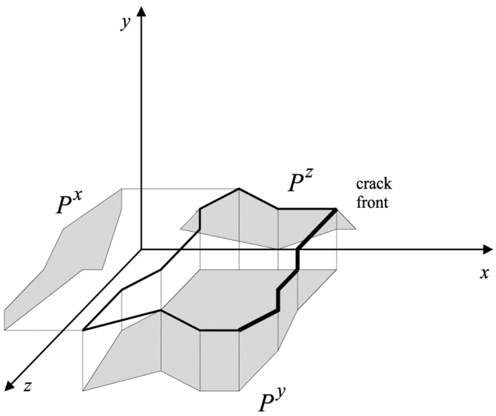

Fig. 2 Geometry of the model

The stable growth of the subcrack within the process zone is simulated as a quasi-continuous process starting at defined front of the long fatigue precrack. Individual intergranular facets adjacent to the crack front are assumed to break gradually in an unstable manner according to prescribed physically justified rules [2]. The geometry of the model is shown in Fig.2. A right-handed Cartesian coordinate system is attached to the cubic zone forming a section of unbounded random tessellation T: the x-axis corresponds to the *crack growth direction*, the z-axis to the macroscopic *direction of the crack front.*

In order to characterize the shape of the fracture surface, several simple numerical characteristics called the roughness indices have been introduced (for details and discussion see [3]). They are based either on the analysis of randomly or systematically selected fracture lines $\boldsymbol{L}$ or on the detailed knowledge of the whole or substantial part of the fracture surface $\boldsymbol{S}$.

Fracture lines

Let $\boldsymbol{S}$ be the fracture surface and $F_{\boldsymbol{v}(y)}$ be vertical planes parallel with the y-axis with the normals $\boldsymbol{v}$. Then $\boldsymbol{L}_{\boldsymbol{v}} = F_{\boldsymbol{v}(y)} \cap \boldsymbol{S}$ are the fracture lines; the natural choice is $\boldsymbol{v}$ along x- and z-axes, then $\boldsymbol{L}_{\boldsymbol{x}}$, $\boldsymbol{L}_{z}$ are approximately parallel with and perpendicular to the crack front, respectively. Let $\|\bullet\|$ denotes the length; then $\|\boldsymbol{L}\|$ and $\|\boldsymbol{P}_{\boldsymbol{u}}(\boldsymbol{L})\|$ are the lengths of $\boldsymbol{L}$ and of its orthogonal projection $\boldsymbol{P}_{\boldsymbol{u}}(\boldsymbol{L})$ into the direction $\boldsymbol{u}$.

The most common characteristic of fracture lines is the *linear roughness* R_L

$$R_L(\boldsymbol{v}) = \frac{\|\boldsymbol{L}_{\boldsymbol{v}}\|}{\|\boldsymbol{P}_{\boldsymbol{v}\times y}(\boldsymbol{L}_{\boldsymbol{v}})\|}.$$

Similarly, the *vertical roughness* R_{LV} is

$$R_{LV}(\boldsymbol{v}) = \frac{\|\boldsymbol{TP}_{y}(\boldsymbol{L}_{\boldsymbol{v}})\|}{\|\boldsymbol{P}_{\boldsymbol{v}\times y}(\boldsymbol{L}_{\boldsymbol{v}})\|},$$

where $\boldsymbol{TP}$ is the total projection. Consequently, $R_{LV}(\boldsymbol{x})$ is the vertical roughness of the fracture line approximately parallel with the crack front and describes the "horizontal overlapping" of the crack front at the distance $x = const.$ from the origin of the crack propagation.

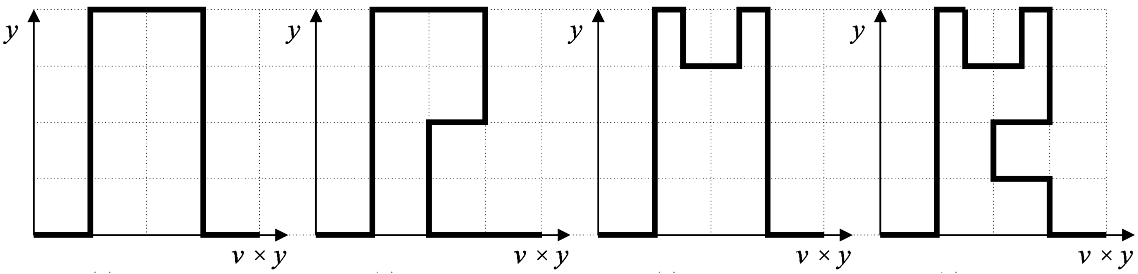

$R_L(\boldsymbol{v}) = 3.00$	$R_L(\boldsymbol{v}) = 3.50$	$R_L(\boldsymbol{v}) = 3.50$	$R_L(\boldsymbol{v}) = 4.00$
$R_{LV}(\boldsymbol{v}) = 2.00$	$R_{LV}(\boldsymbol{v}) = 2.00$	$R_{LV}(\boldsymbol{v}) = 2.50$	$R_{LV}(\boldsymbol{v}) = 2.50$
$R_{LO}(\boldsymbol{v}) = 1.00$	$R_{LO}(\boldsymbol{v}) = 1.50$	$R_{LO}(\boldsymbol{v}) = 1.00$	$R_{LO}(\boldsymbol{v}) = 1.50$

Fig. 3 Roughness indices.

Further, the *index of overlapping* R_{LO} is

$$R_{LO}(\boldsymbol{v}) = \frac{\|\boldsymbol{TP}_{\boldsymbol{v}\times y}(\boldsymbol{L}_{\boldsymbol{v}})\|}{\|\boldsymbol{P}_{\boldsymbol{v}\times y}(\boldsymbol{L}_{\boldsymbol{v}})\|}.$$

The index of overlapping $R_{LO}(\boldsymbol{z})$ characterizes an average "vertical overlapping" along the fracture path $\boldsymbol{z} = const$, i.e. those places where the advancing crack front goes temporarily in the backward direction.

The *profile* or *Behrens roughness* $R_{Lp}(\boldsymbol{v})$ of $\boldsymbol{L}(\boldsymbol{v})$ is defined as the ratio of the mean peak amplitude to the mean peak period and the estimator

$$R_{Lp}(\boldsymbol{v}) = \frac{\Delta y \Sigma p_i}{2 l_t}$$

was proposed in [4]; Δy is the constant (vertical) displacement of a horizontal (i.e. of the direction $\boldsymbol{v} \times \boldsymbol{y}$) test line of length l_t and p_i is the number of intersections $\#(l_t(y \cap \boldsymbol{L}))$. However, $\Delta y \Sigma p_i$ is the estimate of the length of the total vertical projection of such a part $\boldsymbol{P}_y(\Delta \boldsymbol{L}_v)$ that its projection $\boldsymbol{P}_{v \times y}(\Delta \boldsymbol{L}_v)$ has the length l_t. Hence R_{Lp} is equal to $R_{LV}/2$. However, the definition of R_{Lp} clearly elucidates the meaning of R_{LV}.

The linear roughness of an isotropic system of segments is clearly $R_L^{iso} = \pi / 2 = 1.571$ and further $R_{LV}^{iso} = 2R_{Lp}^{ipo} = R_{LO}^{iso} = 1$. The meaning of various indices illustrates Fig. 3.

Fracture surface.
The direct generalization of the above roughness indices concerns the whole fracture surface $\boldsymbol{S}$ or its relevant proportion. The indices then compare the true area of the fracture surface $\|\boldsymbol{S}\|$ or its selected projections with its projection into the mean fracture plane. Let $\boldsymbol{P}^{\boldsymbol{u}}(\boldsymbol{S})$ be the orthogonal projection of $\boldsymbol{S}$ into the plane the normal of which is u. A direct analogy of the linear roughness ($\|\bullet\|$ is the surface content) is the *surface roughness*

$$[R_s]_{\boldsymbol{S}} = \frac{\|\boldsymbol{S}\|}{\|\boldsymbol{P}^y(\boldsymbol{S})\|}.$$

Similarly, the *vertical surface roughness* and *surface overlapping indices* are

$$R_{SV}(\boldsymbol{v}) = \frac{\|\boldsymbol{TP}^v(\boldsymbol{S})\|}{\|\boldsymbol{P}^y(\boldsymbol{S})\|}, \quad R_{SO} = \frac{\|\boldsymbol{TP}^y(\boldsymbol{S})\|}{\|\boldsymbol{P}^y(\boldsymbol{S})\|}.$$

They characterize the "horizontal" (in the direction v) and "vertical" overlapping of the fracture surface, respectively.

The roughness R_S of an isotropic system of (non-overlapping) surface fragments is clearly $R_S^{iso} = 2\pi / \pi = 2$ (the ratio of the surface content of a half-sphere to the area of its equatorial disk). Further, $R_{SV}^{iso} = R_{SO}^{iso} = 1$.

STEREOLOGY OF FRACTURE SURFACE

The estimation of the surface roughness indices of real cracks is very difficult, hence several stereological formuli relating R_S to the indices of fracture lines have been proposed. They are based on simple models of the fracture surface formed *e.g.* by pyramids of different bases *etc.*

The quadratic relations are due to Wright and Carlsson [5] and are supposed to hold for a triangular bases of peaks:

$$\mathrm{I}: \quad R_S = \sqrt{R_{LO}^2 + k^2(R_L^2 - R_{LO}^2)}, \qquad \mathrm{II}: \quad R_S = \sqrt{R_{LO}^2 + k^2 R_{LV}^2}, \quad k = \pi / 2 = 1.571.$$

The same authors proposed also a linear relation (quadratic bases) [6]

$$\mathrm{III}: \quad R_S = R_{LO} + k(R_L - R_{LO}).$$

Coster and Chermant [7] proposed simpler relations valid for fractures without overlapping (*i.e.* $R_{LO} = 1$)

$$\mathrm{IV}: \quad R_S = 1 + k'(R_L - 1), \quad \mathrm{V}: \quad R_S = 1 + R_{LV}, \quad k' = (\pi / 2 - 1)^{-1} = 1.752$$

(the assumed linear relation $R_{LV} = k'(R_L - 1)$ clearly holds exactly for an isotropic fracture line $R_{LV} = 1$ as well as for a flat fracture line $R_{LV} = 0$ and the correct values 2 and 1 are then also obtained for R_S). Finally, Underwood [8] advocates similar formula

$$\text{VI}: \quad R_S = 1 + k''(R_L - 1), \quad k'' = 4/\pi = 1.273.$$

SIMULATION AND ESTIMATION

The tessellations have been produced in a unit cube with the edges corresponding to the chosen coordinate system. The expected number of generated points was 15 000 which is the corresponding cube volume in the unit tessellation. The whole unit cube was intersected by a mesh of 2×99 parallel $F_{\boldsymbol{x}(\boldsymbol{y})}$ and $F_{\boldsymbol{z}(\boldsymbol{y})}$ planes. The vertices of all cell facets, hence also of all fractured facets f_i, are known and their intersections $F_{\bullet(\boldsymbol{y})} \cap f_i$ with each plane of the mesh can be found. Then the length of each fracture line as well as its arbitrary orthogonal and total projections can be exactly calculated. All fracture line indices follow immediately.

The tessellation is corrupted by the edge effects near the cube sides and irregularities of crack propagation occur at the start, end and sides of the crack. Consequently, a protecting 3D frame of the width 0.2 was used and the estimation was limited to the inner cube of the size $0.6 \times 0.6 \times 0.6$.

The obtained results for the index $R_{LO}(\boldsymbol{x})$ are shown in Fig. 4 (note the higher overlapping at the later stages of the crack propagation). The regression lines reveal very roughly the effect of variables x, z on the values of indices - see Tab. 2, where also the corresponding mean values are shown.

Tab. 2 Regression lines, mean values (bold face) and ranges (italics) of fracture line indices

	Bcf0.005		PVT		BePS70	
	x	*z*	*x*	*z*	*x*	*z*
R_L	0.069x+1.43	0.014z+1.34	0.49x+1.38	-0.088z+1.55	0.19x+1.44	-0.49z+1.73
mean	**1.46**	**1.35**	**1.58**	**1.51**	**1.52**	**1.53**
range	*1.1 - 2.1*	1.1 - 2.9	*1.2 - 2.3*	*1.2 - 3.0*	*1.1 - 2.5*	*1.1 - 2.7*
R_{LV}	0.053x+0.80	0.083z+0.71	0.38x+0.76	-0.054z+0.83	0.24x+0.72	-0.41z+0.96
mean	**0.82**	**0.74**	**0.91**	**0.81**	**0.82**	**0.80**
range	*0.4 - 1.4*	*0.4 - 1.7*	*0.5 - 1.4*	*0.4 - 1.7*	*0.4 - 1.6*	*0.3 - 1.5*
R_{LO}	0.025x+1.04	0.084z+1.03	0.23x+1.01	0.060z+1.17	0.035x+1.09	-0.20z+1.23
mean	**1.05**	**1.06**	**1.10**	**1.15**	**1.10**	**1.15**
range	*1 - 1.3*	*1 - 1.8*	*1 - 1.5*	*1 - 2.1*	*1 - 1.7*	*1 - 2.0*

Surface indices have been calculated by combining exact calculations with simple stereological methods. Their values are summarized in Tab. 3 (bold and italic letters denote maximum and minimum values, resp.) and plotted in Fig. 5.

Tab. 3 Surface roughness indices and their coefficients of variation

Tessell.	R_S	CV R_S	$R_{SV}(\boldsymbol{x})$	CV $R_{SV}(\boldsymbol{x})$	$R_{SV}(\boldsymbol{z})$	CV $R_{SV}(\boldsymbol{z})$	R_{SO}	CV R_{SO}
Bcf0.005	*1.54*	**0.11**	*0.63*	**0.19**	*0.67*	**0.20**	*1.02*	*0.033*
PVT	**1.81**	*0.043*	0.74	*0.048*	**0.90**	*0.063*	**1.09**	0.035
BePG70	1.79	0.087	**0.75**	0.11	0.86	0.14	1.08	0.040
BePS70	1.79	0.10	0.71	0.16	0.88	0.14	1.10	**0.069**

Finally, six models of the relation between R_S and fracture line indices R_{LV}, R_{LO} have been compared with the obtained results. For each of n realizations, the values

$$R_L = \sqrt{\overline{R}_L(x).\overline{R}_L(z)}, \quad R_{LV} = \sqrt{\overline{R}_{LV}(x).\overline{R}_{LV}(z)} \quad \text{and} \quad R_{LO} = \overline{R}_{LO}(z)$$

(prime denotes averaging over all x, z values) have been inserted into the model equations in order to obtain the estimates $[R_S(n)]_j$, j = I,II,...,VI, i=1,...,n. Then the mean linear and squared quadratic deviations

$$\Delta_1(j) = R_S - n^{-1}\sum_{i=1}^{n}[R_S(i)]_j, \quad \Delta_2(j) = \sqrt{n^{-1}\sum_{i=1}^{n}\left(R_S - [R_S(i)]_j\right)^2}$$

have been calculated. Tab. 4 presents the results of this comparison (bold face denotes the best model); there were no substantial differences between BePS70 and BePG70 tessellations, hence the both tessellations have been treated together.

Tab. 4 Mean linear (Δ_1) and squared quadratic (Δ_2) deviations of observed and model values.

	I	II	III	IV	V	VI
Bcf0.005 Δ_1	-0.097	0.087	0.069	**0.005**	-0.12	0.15
Δ_2	0.10	0.098	0.071	**0.039**	0.13	0.15
PVT Δ_1	-0.14	0.067	**0.036**	-0.086	**-0.025**	0.11
Δ_2	0.16	0.078	**0.045**	0.11	**0.04**	0.13
BePG70 Δ_1	-0.20	0.063	**0.022**	-0.13	-0.053	0.12
+ BePS70 Δ_2	0.21	0.080	**0.052**	0.15	0.090	0.13

DISCUSSION

Roughness indices of fracture lines

The effect of the variables x, z on the change in the fracture line indices is nearly negligible in quasi-isohedral Bcf0.005 tessellations and much higher in other examined tessellations (Tab. 2). $R_{L\bullet}(x)$ indices grow along the crack path, $R_{\bullet}(z)$ are nearly constant in Bcf0.005 and PVT and markedly decreasing in BePS70. The latter observation suggests an asymmetry in the crack front propagation the origin of which is not clear. The vertical overlapping increases with the growing cell size dispersion. Of special interest is the dispersion of index values shown in Tab. 2 (the rows denoted "*range*"). The particular values have been determined from the fracture lines composed from 30 - 40 segments (facet chords) and the number of independent realizations of the crack was typically 20. Tab. 2 shows that under such sampling conditions, the range of the index value is of the order of 1 and more, the only exception being the index R_{LO}, where the range is narrower in some cases. The distribution of the values is usually asymmetric with a positive skewness and occasionally extremely high values. Such is the situation in stochastically equivalent systems with very simple rules for the crack propagation. As was already noted in [1], the number of facet chords included in the analysis should be of the order of several hundreds in order to obtain a reasonable interval estimate. Consequently, even higher variability of roughness indices can be expected in real materials.

Surface roughness indices

Ratios of maxima to minima have similar values as it was presented in Tab. 1 for R_S. With few exceptions (which may be inaccuracies only), it can be concluded that the maximum values of surface roughness indices and minimum values of their coefficients of variation are attained by cracks in PVT, whereas just a reversed case (minima of indices, maxima of their coefficients of variation) is produced by cracks in nearly isohedral Bcf0.005. Only CV R_{SO} has minimum in Bcf0.005 and maximum (somewhat dubious) in BePS70. Moreover, the differences between indices of PVT and tessellations generated by Bernoulli cluster fields are rather small.

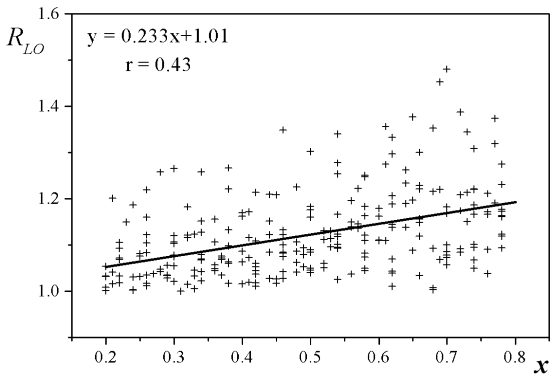

Fig. 4 The values of $R_{LO}(x)$ obtained in 15 realizations of PVT.

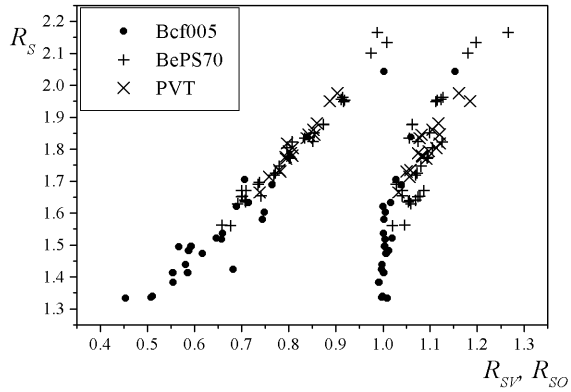

Fig. 5 Relations between indices of surface roughness.

Fig. 5 illustrates the distributions of the index values: nearly the whole range is covered by Bcf0.005 values, indices of tessellations generated by Bernoulli cluster fields are shifted to higher values and PVT indices are restricted to medium range only. A linear relation $R_S \approx 0.53(1 + 3R_{SV})$ seems to hold between R_{SV} and R_S, whereas $R_{SO} > 1$ only when $R_S >\approx 1.6$ ($R_{SV} >\approx 0.7$). Clearly, no vertical overlapping takes place if the vertical roughness is small. Further, the isotropic values of R_S, R_{SV} are only rarely exceeded. The range of surface index values in individual crack realizations with typically 2000 of fractured facets is quite considerable: ≈ 0.7 in Bcf0.005, BePS70, BePG70 tessellations and slightly below 0.5 in PVT. Again, samples of rather great size are necessary even in stochastically equivalent structures with rigid rules of crack propagation. The coefficient of error CE $R_{S\bullet}$ is $\mathrm{CV}R_{S\bullet}/\sqrt{n} \approx (0.05-0.2)/\sqrt{n}$ for n samples of the size ≈ 2000 fractured facets (with the exception of surface indices of vertical overlapping) and higher error values should be expected not only in systems with high cell size dispersion but also in nearly regular grain systems (due to the great effect of crack orientation).

c) Relation between R_S and fracture line roughness indices

The proposed models II and VI can be rejected because the index R_S is seriously underestimated and a strict rejection must be applied also to the model I because of equally serious overestimation (if $\Delta_1 \approx \Delta_2$, which holds in all cases under models I, II, VI, then the bias has the same sign in nearly all cases; if $\Delta_1 << \Delta_2$, the estimates oscillate about the correct value). The plausible explanation of the model failures are the implicit assumptions of isotropy in the model VI and of a high vertical overlapping in the case of quadratic models I, II.

Consequently, only models III, IV and V remain in the play. Strictly speaking, the simple model V is the best one for PVT but a more sophisticated model III taking account of vertical overlapping is nearly equivalent. Because of small differences between index values in PVT and BePG, BePS and also due to a considerable vertical overlapping in the latter two cases, its best validity for cracks in the tessellations generated by Bernoulli cluster field is hardly surprising. Finally, the most simple model IV assuming a direct relation between R_S and R_L describes at best cracks in regular quasi-isohedral Bcf0.005 tessellation. The negligible vertical overlapping in this case is a reasonable explanation of this success demonstrated at best by the smallest observed value of Δ_1 and a great difference between Δ_1 and Δ_2.

As the estimate of surface roughness is nearly exclusively based on the fracture line roughness in the examination of real cracks, the reliability of the considered models is of primary importance and a proper attention will be devoted to this line of study in the next future.

A rather natural objection against the present study can be made, namely that its approach is based on obsolete notions and that a characterization of fracture surfaces by fractal analysis is more appropriate. However, the authors firmly believe that simple characteristics with a straightforward and illustrative geometric interpretation must be preferred in the examination of such complex phenomena as are fracture surfaces in highly variable space filling structures.

ACKNOWLEDGMENT

Research supported by the Ministry of Education of the Czech Republic (contract No. 281100015 - P.P.) and by the Grant Agency of the Czech Republic (contract No. 201/99/0269 - I.S.).

REFERENCES

[1] Saxl, I., Sülleiová, K., Ponížil, P.: 3D Simulations of intergranular fracture. In: L. Parilák (ed.) Proceedings of the International Conference "Fractography 2000", Vysoké Tatry, 15 - 18. 10. 2000. Inst. Mat. Res. Slov. Acad. Sci, Košice 2000, 94-107.
[2] Šandera P, Ponížil P, Pokluda J. In: L. Parilák L (ed.): Fractography 97, Proc Int Conf Vysoké Tatry. Inst. Mat. Res. Slov. Acad. Sci, Košice 1997, 151.
[3] Chermant, J.L.: Précis d'analyse d'images. Presses du C.N.R.S., Paris 1989.
[4] Underwood, E.E.: In: J.H. Steele (ed.): Practical applications of quantitative metallography. ASTM STP 839. Philadelphia 1983.
[5] Wright, K., Karlsson, B.: J. Microscopy, 130 (1983), 37.
[6] Wright, K., Karlsson, B.: In: Stereol. Iugosl. 3 (1981), Suppl. 1, 247.
[7] Coster, M., Chermant, J.L.: Int. Met. Rev. 28 (1983), 228.
[8] Underwood E.E.: J. Metals 38 (1986), 30.